Available online at www.sciencedirect.com
SCIENCE DIRECT
Catalysis Today 105 (2005) 206–222
CATALYSIS TODAY
www.elsevier.com/locate/cattod

Nonlinear dynamics on catalytic surfaces

R. Imbihl *

Institut für Physikalische Chemie und Elektrochemie, Universität Hannover, Callinstrasse 3-3a, D-30167 Hannover, Germany

Abstract

Recent progress in nonlinear dynamics on surfaces is reviewed focusing on selected examples from single crystal studies. Complex patterns, fluctuations in small scale systems, and controlling catalytic reactions by microstructured heating or through local heating with a laser beam are some of the issues to be discussed.

Keywords: Nonlinear dynamics; Complex patterns; Catalytic reactions

1. Introduction

When the first experimental observation of rate oscillations in a catalytic reaction was reported by the group of Wicke in 1970 [1], this phenomenon almost immediately aroused the interest of scientists and numerous hypothetical mechanisms were proposed [2]. It soon became evident that the rate oscillations were the result of a selforganization process on the catalytic surface and that surface analytical tools and well-defined experiments and catalysts were required for understanding the mechanism behind the oscillatory kinetics [3–12]. Today the mechanistic aspect in these studies has almost completely vanished and the emphasis has shifted instead to controlling spatiotemporal pattern formation and to the development and application of spatially resolving in situ techniques that come close to atomic resolution. This situation reflects the enormous progress which has been made due to the concept of low pressure single crystal studies.

The purpose of this short review is not so much to give an overview of the individual reaction systems and the different subfields – this can be found in some older review articles [3–12] – but to demonstrate with a few selected topics the current status in the development of this field. Despite all the progress, which has been achieved in the detailed mechanistic understanding, there are still a number of questions, which are difficult to answer and which, to a certain degree, remain unsolved. This is first of all the question of the significance of the results in real catalysis. Secondly, the question whether and to what extent the results obtained in low pressure single crystal studies can be extrapolated to explain the oscillatory behavior at high pressure and with polycrystalline catalysts also remains difficult to ascertain. The classical pressure and material gap problem of heterogeneous catalysis is thus also present in the oscillation studies and its bridging remains a challenging task.

2. Mechanisms of oscillations and pattern formation

2.1. Basic requirements

Practically by definition heterogeneously catalyzed reactions are systems far from thermodynamical equilibrium. Kinetic oscillation and spatiotemporal pattern formation can develop in such systems and before they were investigated on catalytic surfaces these phenomena had already been extensively studied with liquid phase reaction systems, the most well known example being the Belousov-Zhabotinskii reaction [13,14]. The theoretical framework for understanding these phenomena have been developed in a branch of physics and mathematics, which is termed nonlinear dynamics. The name reflects the fact that the underlying mathematical equations have to be non-linear in order to exhibit this type of behavior.

* Fax: +49 511 762 4009.
E-mail address: imbihl@mbox.pci.uni-hannover.de.

0920-5861/$ – see front matter © 2005 Elsevier B.V. All rights reserved.
doi:10.1016/j.cattod.2005.02.045

Similar to liquid phase reactions the general structure of the mathematical equations describing spatiotemporal pattern formation on surfaces is that of a reaction–diffusion (RD) system. We can write such an RD system in the form

$$x_i = F_i(x_j, \lambda) + \Delta_i \nabla^2 x_i \quad (1)$$

where x_i represents a variable, in our case the adsorbate coverage of species $i - \lambda$ stands for a set of parameters, e.g. partial pressure and temperature. The (non-linear) local reaction kinetics are contained in the expression F_i, while the second term represents the diffusion of species where, for simplicity, we have assumed simple Fickian diffusion. If the surface reacts spatially homogeneously the diffusion term vanishes and our system can be described by a set of ordinary differential equations (ODE's). If we therefore neglect the aspect of pattern formation, i.e. we assume a spatially uniformly oscillating surface, we discuss the mechanism in terms of a point model of ordinary differential equations (ODE's) representing the local reaction kinetics.

2.2. Oscillation mechanisms

In the review of oscillatory surface reactions by Schüth and Schmidt about 60 oscillatory reaction systems are listed [8]. Apparently, the mechanistic requirements for obtaining oscillatory behavior are not very restrictive and there has even been some speculation whether most, if not all, catalytic reactions exhibit oscillatory behavior in some parameter range. For most of the systems no detailed mechanistic investigations have been made. Detailed studies have been carried out for the reactions of the automotive catalytic converter, namely, catalytic CO oxidation and catalytic NO reduction, which are investigated on platinum, palladium, and rhodium surfaces. The mechanism may change depending on the reaction conditions. For the low pressure experiments of catalytic CO oxidation on platinum single crystal surface the phase transition model has been verified by experiment [15] while at high pressure ($p > 1$ mbar) an oxidation/reduction mechanism is supported by experimental data [16,17].

In the following a short overview of the mechanisms is given, which are well supported by experimental data and realistic mathematical modeling. For details the reader is referred to several review papers and references therein [5–10].

2.2.1. Catalytic CO oxidation

2.2.1.1. The surface phase transition model. The clean surfaces of Pt(1 0 0) and Pt(1 1 0) exhibit a reconstruction which can be reversibly lifted upon adsorption [6,7,10]. An adsorbate-induced surface phase transition between the clean reconstructed surface and the adsorbate-covered bulk-like (1×1) surface is thus constituted, which is controlled by a critical adsorbate coverage. Since oxygen adsorption on Pt surfaces is highly structure sensitive the phase transition is associated with a change in the oxygen sticking coefficient and thus with a change in catalytic activity.

The basic principle of the oscillation mechanism in catalytic CO oxidation on Pt(1 1 0) can be demonstrated with the help of Fig. 1. Starting with the CO-covered 1×1 surface the high reactivity will decrease the CO coverage until below a critical CO coverage the surface reconstructs into the less active 1×2 phase. On this phase CO adsorption dominates over O_2 adsorption and the CO coverage grows until beyond the critical CO coverage the active 1×1 is established again.

2.2.1.2. The oxidation–reduction model. Pd surfaces are insofar different from Pt as oxygen can more easily penetrate into the Pd bulk and oxide formation is facilitated. Moreover, the clean surfaces do not reconstruct. It has been demonstrated that even at low p ($p < 10^{-3}$ mbar) oxygen can penetrate reversibly into subsurface sites of Pd(1 1 0) thus lowering its catalytic activity [18]. This subsurface oxygen formation can give rise to oscillatory behavior because on the inactive CO covered surface the subsurface oxygen reservoir is depleted through segregation to the surface, followed by reaction with CO, thus restoring the catalytic activity of the Pd(1 1 0) surface. With the active

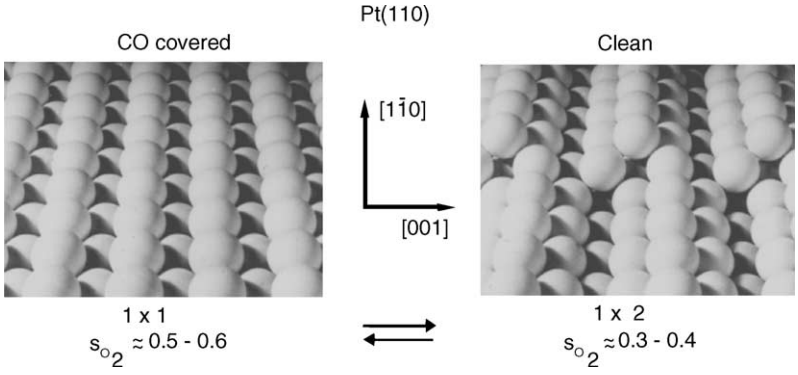

Fig. 1. Ball model illustrating the CO induced $1 \times 1 \rightleftarrows 1 \times 2$ surface phase transition of Pt(1 1 0). The different oxygen sticking coefficients, s_{O_2}'s, of the two phases are responsible for rate oscillations during catalytic CO oxidation. The model also demonstrates how the necessary mass transport of Pt atoms creates an atomic step on the surface.

surface being covered by oxygen the filling of the subsurface oxygen reservoir begins again, completing the oscillatory cycle.

The subsurface oxygen species of Pd(1 1 0) observed at low p is still distinctly different from a true bulk oxide. One can, however, expect that at higher p the subsurface oxygen phase transforms into a true Pd oxide,. The mechanism of rate oscillations in CO oxidation at atmospheric pressure on polycrystalline Pd, Ir, and Pt has been attributed to a periodic oxidation and reduction of the surface as first proposed by Sales, Turner, and Maple [19]. Experimental proofs that such an oxidation–reduction mechanism is in fact operating were provided for Pt supported on SiO_2 by in-situ X-ray diffraction and for supported Pd catalysts by X-ray absorption spectroscopy [16,17].

2.2.2. Catalytic NO reduction

2.2.2.1. The vacancy model. The oscillations, which arise in the NO + CO reaction on a Pt(1 0 0) surface have been extensively studied [6,10,20]. It has been shown that a minimum oscillator can be constructed from the vacant site requirement for NO dissociation. This requirement gives rise to an autocatalytic behavior with respect to the number of vacant sites (*), according to

$$NO_{ad} + CO_{ad} + * \rightarrow 1/2N_2 + CO_2 + 3*$$

Under certain conditions the surface phase transition $(1 \times 1) \leftrightarrow$ hex is involved in the oscillations but presumably its role lies mainly in synchronizing the different oscillating parts of the surface [20–23]. Mechanistically very similar are two other oscillatory reactions on Pt(1 0 0) involving NO, namely the $NO + H_2$ and the $NO + NH_3$ reaction [24].

2.2.2.2. The adlayer displacement model. NO dissociates easily on Rh surfaces but the dissociation products N_{ad} and O_{ad} repel each other so that the more strongly bonded oxygen can displace a nitrogen adlayer, which is forced to

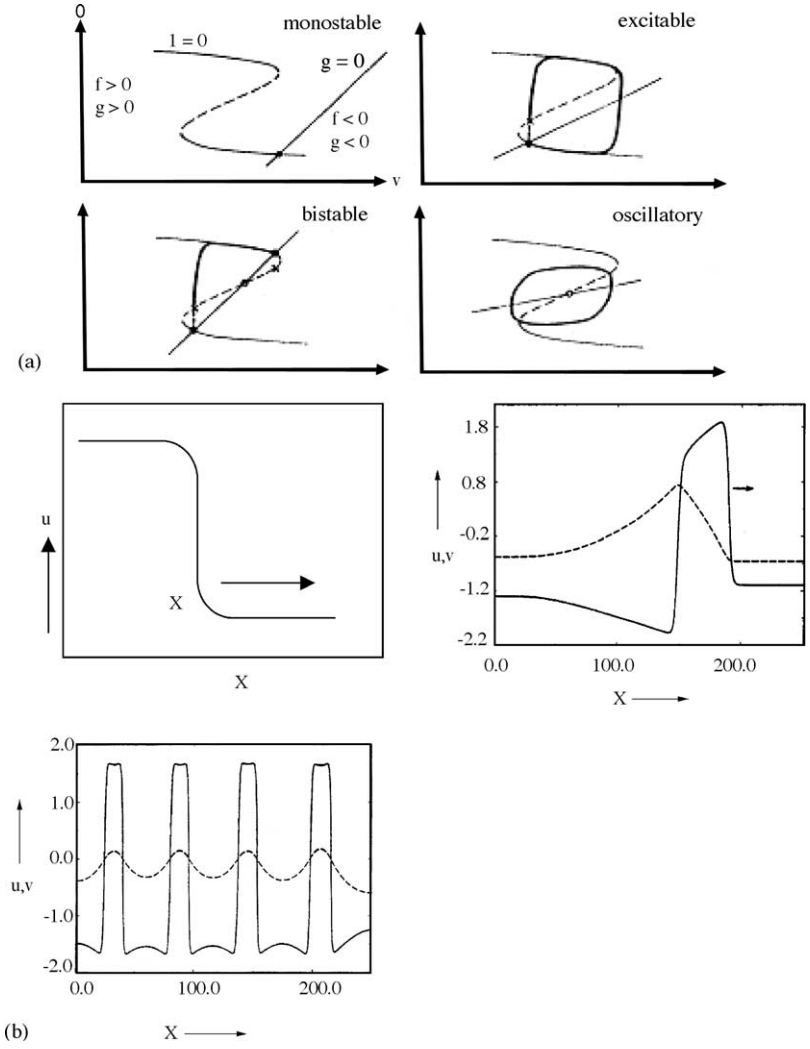

Fig. 2. Basic solutions of an activator-inhibitor model given here by the FitzHugh-Nagumo equations. (a) Different types of stationary points in the ODE model given here by the intersection of the two nullclines, $f(u,v) = 0$ and $g(u,v) = 0$. Monostable, bistable, excitable and oscillatory behavior. (b) Basic 1D-solutions of the RD system showing fronts, pulses, and stationary (Turing) patterns.

desorb. This happens on Rh(1 1 0) and Rh(1 1 1) where rate oscillations and a large variety of different chemical wave patterns have been found [25–28]. In agreement with the proposed mechanism no oscillations were found on Rh(1 0 0) where the nitrogen adlayer is bonded much stronger. Mathematical modeling based on the experimentally determined repulsive interaction between N_{ad} and O_{ad} can reproduce quite in detail the experimentally determined phase diagram for Rh(1 1 0)/NO + H_2 (see below) [27,28].

2.3. Chemical wave patterns

A large part of the dynamic behavior we observe in chemical reaction systems can be understood in terms of a simple 2-variable model with one species (u) called activator and the other species (v) called inhibitor [13]. The most well known of these activator-inhibitor models is the so-called FitzHugh-Nagumo model:

$$\frac{du}{dt} = \frac{1}{\varepsilon}\left(u - \frac{u^3}{3} - v\right) + D_u\nabla^2 u = f(u,v) + D_u\nabla^2 u \qquad (2)$$

$$\frac{dv}{dt} = u + b - av + D_v\nabla^2 v = g(u,v) + D_v\nabla^2 v \qquad (3)$$

The stationary solution is given by the intersection of the two nullclines obtained by setting $f(u,v) = 0$ and $g(u,v) = 0$. One obtains, besides the trivial case of monostability, three types of solutions – bistability, excitability, and oscillatory behavior – which are visualized by the nullclines in Fig. 2a. The different types of local behavior correspond to different types of spatiotemporal solutions, which are depicted in Fig. 2b. In a bistable system reaction fronts initiate transitions between the two stable states. In an excitable system a sufficiently large perturbation causes the propagation of a pulse which, in a 2D-system, corresponds to a spiral wave or, if a trigger center is present, to a target pattern. Finally, if the inhibitor diffuses much more rapidly than the activator a stationary concentration pattern may develop commonly known under the name ''Turing-structure''.

It should be added that the structure of the RD equation given by Eq. (1) is strongly simplified. Diffusion on single crystal surfaces is in general not isotropic and, moreover, interactions between the adparticles are present, which give rise to strong deviations from Fickian diffusion. Besides the local coupling, represented by the diffusion term, often an additional global coupling is present, which is transmitted via the partial pressure changes in the gas phase arising due to mass balance in a reactor. All these modifications result in new types of spatiotemporal patterns, which occur only on surfaces but not in liquid phase reactions. There diffusion is isotropic and energetic interactions between the reacting species are absent or very small.

The standing waves and cellular patterns, which are seen during catalytic CO oxidation on Pt(1 1 0), have to be attributed to global coupling [7,10,29–31]. In the system

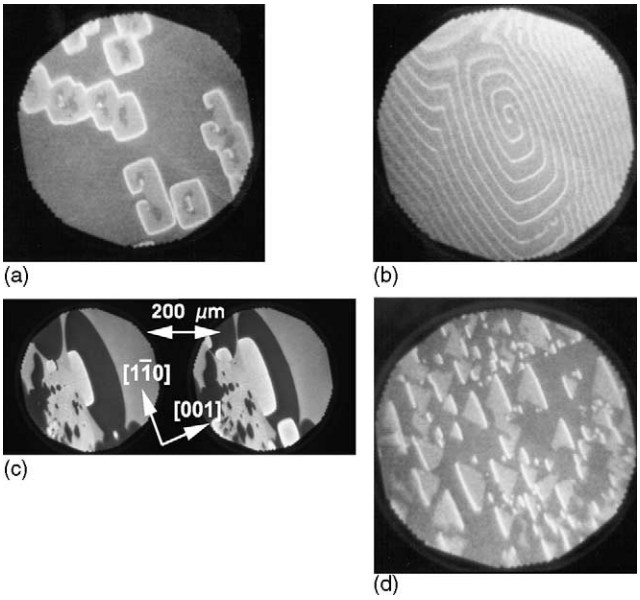

Fig. 3. PEEM images demonstrating different geometries of chemical wave patterns in the NO + H_2 reaction on Rh(1 1 0). The diameter of the imaged area varies between 300 and 400 μm. The crystallographic axes indicated in (c) refer to all images. Experimental conditions: $T = 620$ K, p_{NO} and p_{H_2} vary in the 10^{-6} mbar range. (From refs. [25–28]). (a) Rectangular target patterns. (b) Rectangular spiral wave. (c) Simultaneous presence of elliptical and rectangular front geometries in the region of dynamic bistability. (d) Travelling wave fragments.

Rh(1 1 0)/NO + H_2 the presence of several adsorbate-induced reconstructions with different anisotropies gives rise to a state-dependent diffusional anisotropy. This state-dependent anisotropy gives rise to new types of wave patterns such as rectangularly shaped target patterns and spiral waves as well as travelling wave fragments shown in Fig. 3 [25–28]. The fact that the experimentally determined bifurcation diagram can be well reproduced with a mathematical model as shown in Fig. 4 demonstrates that even chemically complex systems are now mechanistically well understood. The structure sensitivity of reactions like the NO reduction with CO on Pt has been exploited by using chemical wave patterns as a means for detecting surface topographical changes. Such changes occur as a Pt(1 0 0) single crystal is mechanically deformed in front of a photoelectron emission microscopy (PEEM) optics [32]. The surface defects which are created destroy the target patterns, transforming the fragments into spiral waves, which are pinned at the defects.

So far we have not distinguished between single crystal experiments conducted under isothermal conditions at low pressure ($p < 10^{-3}$ mbar) and the high pressure experiments ($p > 1$ mbar) carried out with polycrystalline material. Such a distinction is, however, essential because at high p the reaction is no longer isothermal and thermal coupling may easily prevail. In addition, heat and mass transport effects can no longer be neglected but may dominate the behavior of the whole reaction system.

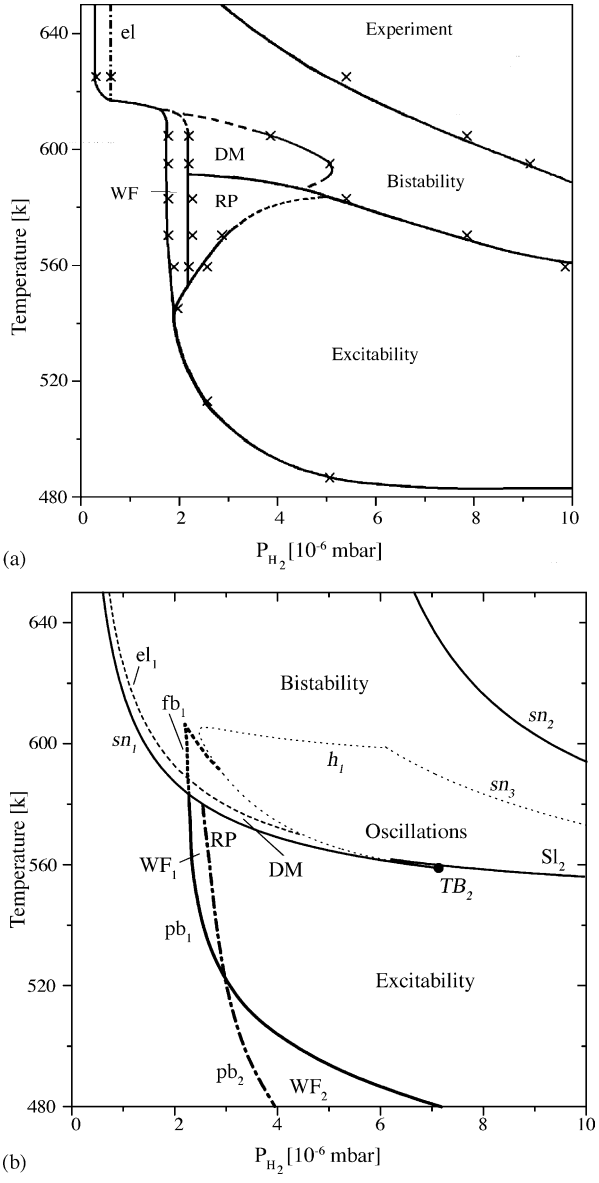

Fig. 4. Comparison between experimental and simulated bifurcation diagram. The regions where different types of spatial patterns formation occur are shown in the (p_{H_2}, T)-plane at fixed $p_{NO} = 1.6 \times 10^{-6}$ mbar. Abbreviations: RP = rectangular patterns, WF = wave fragments, DM = double metastability, el = equistability line. For a more complete description see ref. [28]. (a) Experimental bifurcation diagram (From ref. [27]). (b) Calculated bifurcation diagram for the reaction–diffusion model. (From ref. [28]).

3. Complex patterns due to additional chemical species or substrate modifications

3.1. Subsurface oxygen formation

Quite surprisingly, a number of different pattern forming surface reactions exhibited a common feature irrespective of the catalytic reaction, the metal substrate or the surface orientation. Under certain conditions when two reaction fronts underwent a collision, in PEEM the formation of a very bright spot in the collision area was visible [30,33–36]. The brightness of this spot corresponds to a work function lowered by up to 1 eV with respect to the level of the clean metal surface. The enhanced brightness has been attributed to the formation of the subsurface oxygen which means that despite the pressure still being far below the thermodynamical limit for formation of a stable oxide reaction conditions can enforce the penetration of oxygen into the deeper layers of a metal. The formation of such regions with an enhanced brightness is depicted by the PEEM images in Fig. 5a recorded during the $O_2 + H_2$ reaction on Rh(1 1 1) [33]. If the Rh(1 1 1) surface is exposed to a large dose of oxygen a (8×8) surface oxide forms whose titration with hydrogen leads to triangularly shaped fronts as depicted in Fig. 5b and c [36]. The triangular shape has been explained as being due to the three-fold symmetry of the bulk.

The first observation of subsurface oxygen formation in pattern forming reactions has been with catalytic CO oxidation on Pt(1 0 0) and Pt(1 1 0) [30,35]. Subsequently, the same phenomenon has also been found in the $NO + H_2$ and the $O_2 + H_2$ reaction on Rh single crystal surfaces [33,34]. At this point it should also be clarified that so far no real spectroscopic or structural characterization of this species exists. With photoelectron diffraction the population of subsurface site has been proven during the adsorption of oxygen on Rh(1 1 1) but it remains to be shown that this species is identical with the species which is responsible for the low work function areas in pattern forming systems [37]. Indirect evidence is, however, conclusive enough to deduce that a new state of oxygen with negative dipole moment must have been formed, leaving the precise location of this species open.

For the system Pt(1 1 0)/$CO + O_2$ this newly discovered species solved a longstanding problem. For this system a kind of standard model consisting of three variables exists, which effectively reduces to only a two-variables model of the FitzHugh-Nagumo type because of the three variables – the CO and the oxygen coverage plus a variable describing the surface reconstruction – two, the CO and the oxygen coverage, are strictly anti-correlated and therefore not independent. All elementary types of pattern like target pattern or spiral waves could be well reproduced but problems arose with the standing wave patterns seen on Pt(1 1 0) [7,10,29].

Simulations predicted standing waves but superimposed on a homogeneously oscillating background and the standing wave patterns were only stable in a tiny region of parameter space [29]. With subsurface oxygen as an effective third variable the standing waves could be reproduced as demonstrated in Fig. 6 [30]. The essential mechanism is the reflective collision of pulses, i.e. the subsurface oxygen survives the collision long enough to trigger the nucleation of new pulses. Global coupling via the gas phase is required to ensure a robust pattern which otherwise would be destroyed by unavoidable inhomogeneities of the surface. Alternative mechanisms, for example, by

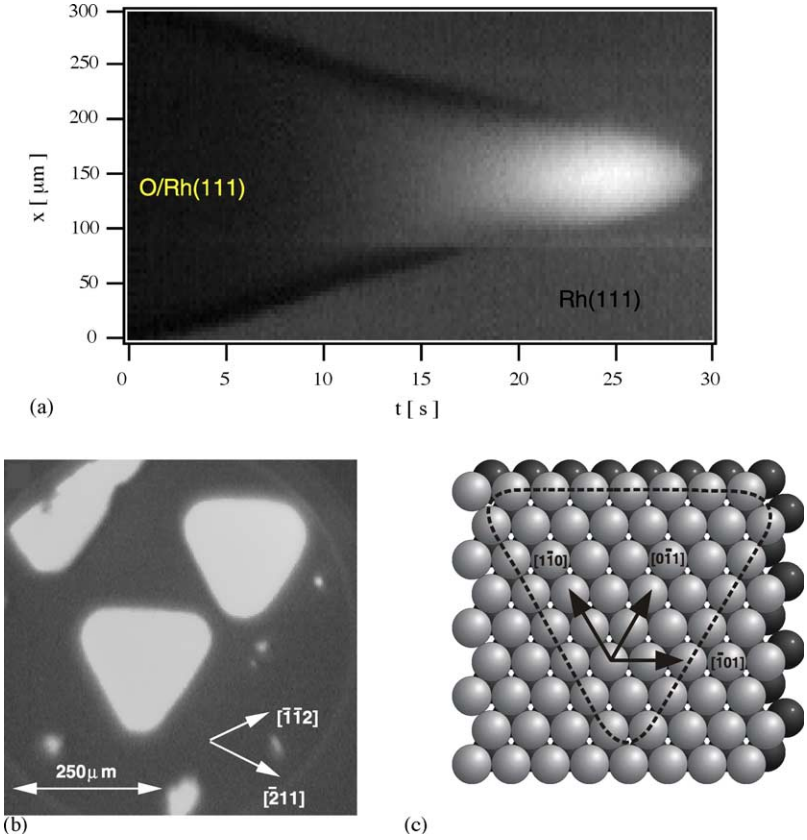

Fig. 5. Influence of subsurface oxygen and of a surface oxide on reduction fronts in the $O_2 + H_2$ reaction on Rh(1 1 1). (a) *x–t*-Diagram demonstrating how the formation of a low WF area in between two colliding fronts leads to reduction of the front velocity. The *x–t*-diagram was constructed by taking PEEM intensity profiles in a direction perpendicular to the front line. Experimental conditions: pretreatment of the sample with oxygen for t_{OX} = 40 h; prior to the titration 160 L O_2 exposure was applied; titration at T = 450 K with $p_{H_2} = 4 \times 10^{-7}$ mbar. (From ref. [33]). (b) PEEM images showing a triangular front geometry during the titration of the (8 × 8)-O structure on Rh(1 1 1) with hydrogen ($p_{H_2} = 5.6 \times 10^{-7}$ mbar) at T = 480 K. The (8 × 8)-O structure was prepared by exposing the Rh(1 1 1) surface at T = 770 K to $p_{O_2} = 2 \times 10^{-4}$ mbar for 1 h. (From ref. [36]). (c) Relation between the front geometry in (b) to the surface crystallography.

a stochastic resonance, have been proposed but lack experimental support [38].

3.2. Reactive phase separation

Alkali metals are well known as so-called electronic promoters in a number of industrially important catalytic reactions [39]. They are very reactive and very mobile on transition metal surfaces and the question therefore was, whether this species is part of the spatiotemporal dynamics of a catalytic reaction. The system Rh(1 1 0)/$O_2 + H_2$ exhibits bistable behavior. With predosed potassium one still observes reaction fronts but these fronts are now transporting potassium as shown in Fig. 7 [40–46]. With progressive enrichment of potassium in the front region the reaction fronts slow down until finally a stationary pattern is formed in which potassium and oxygen are condensed into islands of macroscopic size as shown in Fig. 7.

If one starts the experiment from reducing conditions, a quite regular structure is obtained, which bifurcates from the spatially uniform state, as required for a Turing structure [43,46]. Calling the pattern a Turing structure would nevertheless be misleading, because the essential driving force for the condensation process is the strong chemical affinity between oxygen and the alkali metal and not the different diffusion rate of an activator and inhibitor as in the original definition of Turing. As shown by realistic mathematical modeling and by an analysis with a general model the energetic interactions are in fact the main driving force for the development of a stationary pattern [43,44]. Accordingly, the term reactive phase separation appears to be more appropriate. Phase separation is of course something, which exists already in equilibrium thermodynamics but the effect of the reaction is that a length scale is introduced.

The concept of reactive phase separation is not all restrictive and it applies in principle to any bimetallic catalytic surface where one component is mobile and undergoes a strong energetic interaction with one of the reactants. Naturally, first other alkali metal promoted reactions were investigated and similar effects as in the system described above were found in Rh(1 1 0)/Pt/K/$O_2 + H_2$ [45], in Rh(1 1 0)/K + Cs/$O_2 + H_2$ [46], and in Rh(1 1 0)/K/NO + H_2 [47]. In the mixed K + Cs alkali layer on Rh(1 1 0) a macroscopic phase separation of the two alkali layers in addition to the formation on alkali rich and on

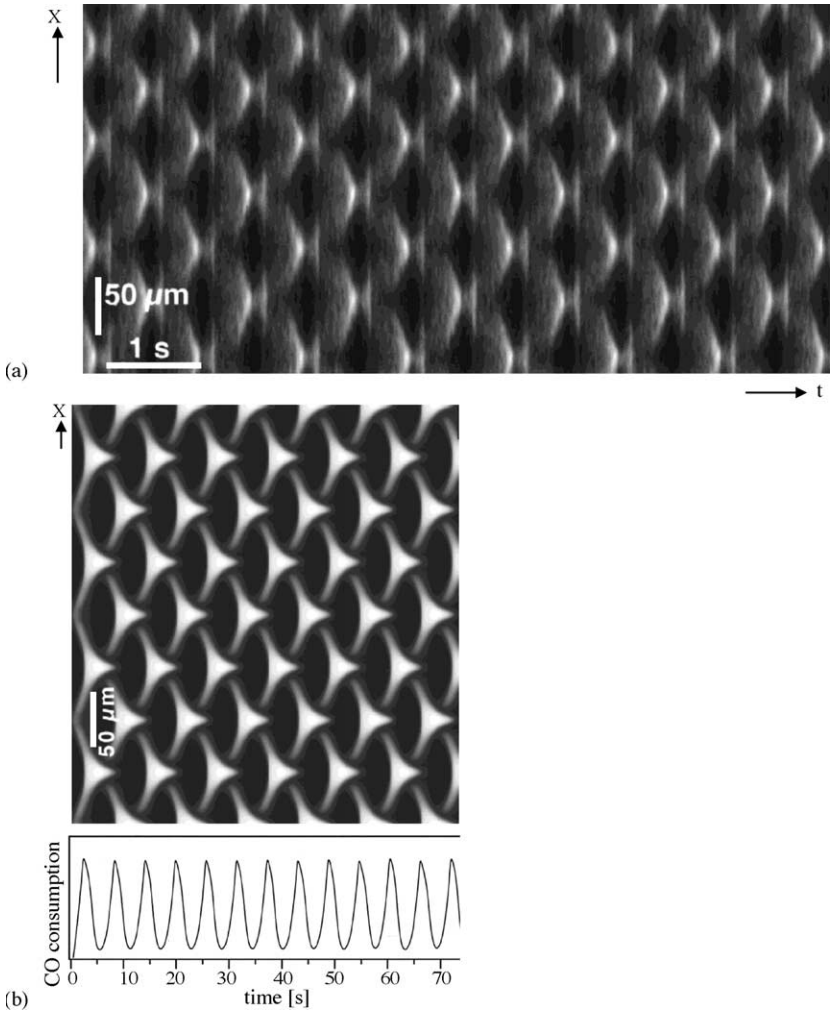

Fig. 6. Standing waves in catalytic CO oxidation on Pt(1 1 0). Experiment and simulation. (From ref. [30]. Reproduced with permission of the authors). (a) Experiment: space-time diagram of standing waves. The time interval shown is 16 s, the cross section length is 346 μm. Parameters: $T = 564$ K, range 10^{-4} mbar. (b) Experiment: space–time diagram of the calculated PEEM intensity in a one-dimensional simulation of pattern produced by repeated reflecting wave collisions. The time interval shown is 70 s.

alkali poor phase were found [46]. In the NO + H_2 reaction on Rh(1 1 0)/K the system retained its excitability with potassium but the pulses were now dragging along potassium [47].

3.3. Reaction-induced substrate modifications

As demonstrated with Fig. 1 the different densities of surface atoms in the 1×1 and 1×2 "missing row" reconstruction of Pt(1 1 0) requires that the $1 \times 1 \leftrightarrow 1 \times 2$ surface phase transition is associated with the mass transport of 50% of the surface atoms. This necessarily causes a roughening of the Pt(1 1 0) surface which, under suitable conditions, may even turn into a (micro)facetting of the surface [48–55]. A stationary (Turing-like) pattern may develop, in which microfacets of equal orientation are arranged such that they form a regular sawtooth-like array of facets with a lateral periodicity of ≈200 Å [49,50]. With LEEM it was demonstrated that despite the microscopic mechanism of the phase transition on Pt(1 1 0) the reaction-induced topographical surface changes in CO oxidation can reach macroscopic dimensions thus establishing a bridge to the morphological changes seen with real catalysts [55].

Fig. 8 shows the development of a periodic facet pattern in a Monte Carlo simulation of catalytic CO oxidation on Pt(1 1 0) starting from an initially flat surface [52]. The kinetic Monte Carlo simulation was used to mimic the movement of individual Pt atoms under reaction conditions. Since the roughening of a Pt(1 1 0) surface is reversible and depends on the reaction conditions or, more precisely on the history of chemical waves, which passed over a certain area, the roughening/facetting process becomes part of the spatiotemporal dynamics of the reaction. Complex patterns can form due to this memory effect as is demonstrated in Fig. 9, showing the development of a kind of channel structure on the Pt(1 1 0) surface under reaction conditions [53]. The sides of the channel are formed by roughened Pt(1 1 0) surface (dark area) and inside the channel oxygen

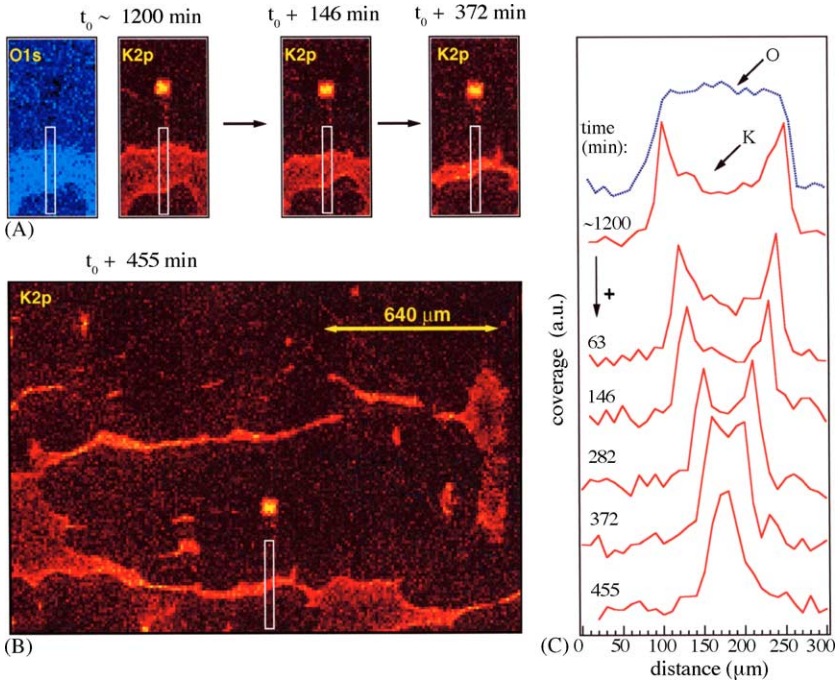

Fig. 7. Potassium and oxygen distribution in the final stages of the condensation process, starting from ~1200 min after ignition of the reduction fronts. Brighter gray levels reflect higher count rates, i.e. higher concentrations. (A) O 1s image and a series of K 2p images (320 μm × 640 μm) showing the coalescence of two reaction fronts. White rectangles mark the windows used for the intensity profiles reproduced in (C). The crystallographic [1 1 0]-direction of the Rh(1 1 0) surface is parallel to the vertical direction as in (B). The bright feature in the K 2p images is a square-shaped Pt patch acting as easy detectable nucleation center. (B) Large scale K 2p image showing a practically stationary K distribution after condensation has reached its final stage. (C) O and K coverage profiles taken along the rectangular window indicated in (A). Experimental conditions: $T \approx 550$ K, $p_{O_2} = 1.9 \times 10^{-7}$ mbar, $p_{H_2} = 0.8 \times 10^{-7}$ mbar. (From ref. [40]).

pulses (bright spots) propagate. Since, on one side the catalytic activity of the Pt(1 1 0) surface is modified by roughening while, on the other side, both roughening and thermal reordering depend on the adsorbate coverages, apparently a rather complex system of possible feed back mechanisms exists, which can generate unusual and complicated patterns. As an example we can consider the rotating ''soliton-like'' travelling wave fragment, which is observed as a transient during catalytic CO oxidation on a strongly roughened Pt(1 1 0) surface [54].

4. Design and control of catalytic surfaces

4.1. Microstructured surfaces

Real catalysts are typically structurally and chemically complex systems built up of several components. For exploring the synergetic effects, which can be reached by optimizing the composition and preparation of a multi component catalyst, one has to understand the diffusional coupling between differently reactive phases. As a model system for studying such transport effects one can construct microstructured bimetallic surfaces by optical lithography [56–67]. By varying the size and the geometry of differently reactive domains one has control over the diffusional coupling between the differently active components [60,61]. One could think of catalyst optimization by design but such a ''microchemical engineering'' of a catalyst is still more a concept in basic research than an alternative route for building better catalysts in industrial applications.

On catalytic surfaces the use of photolithography for creating microstructured surfaces has the great advantage that the length scale of the structures and chemical wave patterns just falls in the right range to allow an in-situ imaging with photoelectron emission microscopy (PEEM). With electron beam lithography structures down to ≈100 Å resolution can be generated but no simple in-situ techniques are available to image the surface in this range [68]. With the development of nanotechnology today also a number of chemical techniques are available to create nanostructured surfaces such as block copolymerization but the inherent disadvantage remains that in general only the integral catalytic behavior can be followed during reactions [69].

With microstructured surfaces nearly exclusively the reaction systems of the automotive catalytic converter have been studied. Catalytic CO oxidation, the $O_2 + H_2$ reaction and NO reduction with CO or H_2 were investigated in the 10^{-7}–10^{-3} mbar range on Pt, Rh, and Pd style crystal surfaces microstructured by deposition of Ti, Pd, Rh, Pt, and Au [56–67]. The experiments were accompanied by extensive simulations.

With Ti deposited on some active material, one essentially restricts the size of the active area because under reaction conditions the Ti is rapidly converted to unreactive TiO_2. One can thus study the influence of size and

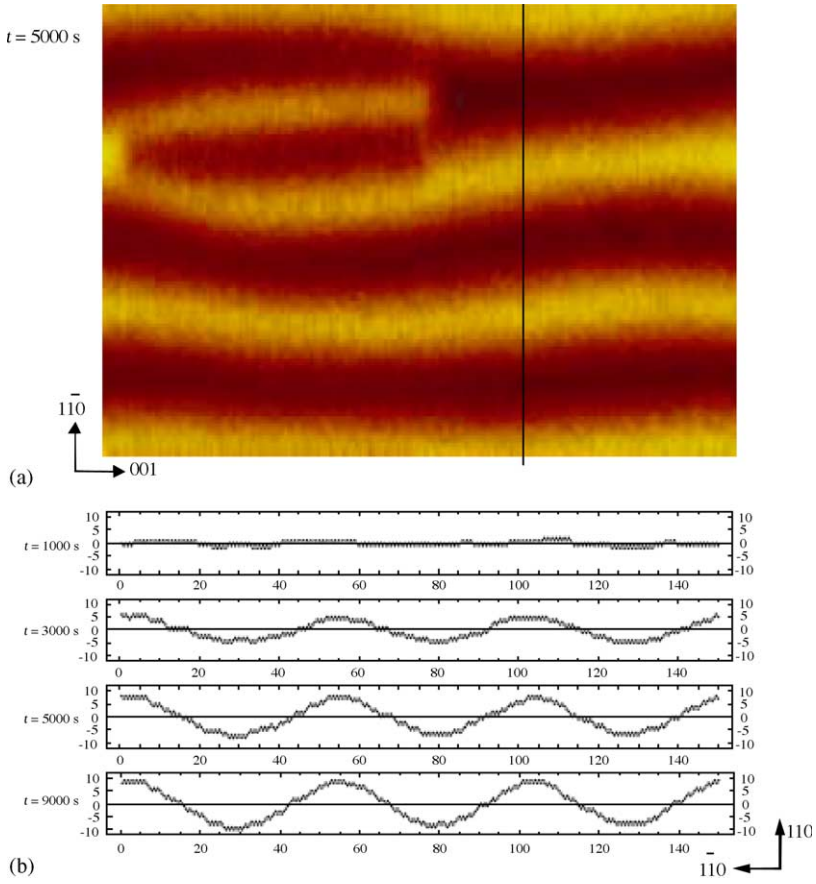

Fig. 8. Monte Carlo simulation of the formation of regularly spaced facets during catalytic CO oxidation on a Pt(1 1 0) surface. (From ref. [52]). Facetted surface of 150 atoms × 150 atoms dimension with the elevated parts being marked by a brighter gray level. (a) Changes in the surface profile during the development of facetting. The surface sections at different time moments were taken in the $[1\bar{1}0]$ direction as shown by the line in (a). (b) The periodicity of 50–60 lattice units in the $[1\bar{1}0]$ direction corresponds to 14–17 nm.

geometry on pattern formation or guide waves through narrow channels [64–66]. Geometry effects in front nucleation were seen [58]. Catalytically more interesting is the deposition of a second metal with different activity because the diffusional coupling can give rise to interesting dynamic effects [60–63,67]. Controlled front nucleation at interfaces, a size dependent reactivity and geometry effects in the nucleation and in the propagation of chemical waves have been found.

Fig. 10 shows the titration of an oxygen covered microstructured Pt(1 0 0)/Rh surface with hydrogen [60]. The PEEM images show how first two reaction fronts nucleate at the perimeter of two differently sized Pt(1 0 0) circles. The reaction fronts spread out into the surrounding Rh surface while the Pt circles themselves remain still oxygen covered for some time. One notes that first the small circle becomes bright (oxygen free) while the larger one follows with a delay of ≈1 min. The difference in reactivity can be attributed to the stronger diffusional coupling of the smaller circle because the amount of hydrogen, which diffuses back from the Rh surface into the Pt circle, will be proportional to the perimeter, i.e. proportional to r, whereas the amount of oxygen to be reacted away is proportional to r^2.

Despite its appealing simplicity the concept of microstructured surfaces has so far only been applied to a small class of reaction systems, the reactions of the automotive catalytic converter, which take place on noble metal catalysts. One problem is of course that the limited stability of the metal film excludes cleaning by extensive sputtering or high temperature annealing. A second problem is that the PEEM method requires $p < 10^{-3}$ mbar, a condition, which excludes most of the catalytically interesting reactions. A third problem is that PEEM primarily images the work function and therefore yields little or no information about the identity of the imaged species. Chemically complex systems are therefore not suitable for PEEM. This limitation, however, can be overcome by scanning photoelectron microscopy (SPEM) – a technique, which uses synchrotron radiation to excite core level electrons, thus being element sensitive [70]. It was shown with SPEM that the stationary concentration patterns, which developed during the $O_2 + H_2$ reaction on a microstructured Rh(1 1 0)/Pt sample were in fact due to the presence of potassium as contaminant [45,59,67]. The primary pattern forming step in this system was shown to be caused by the condensation of potassium and oxygen into macroscopic islands as described in Section 3.2 [45].

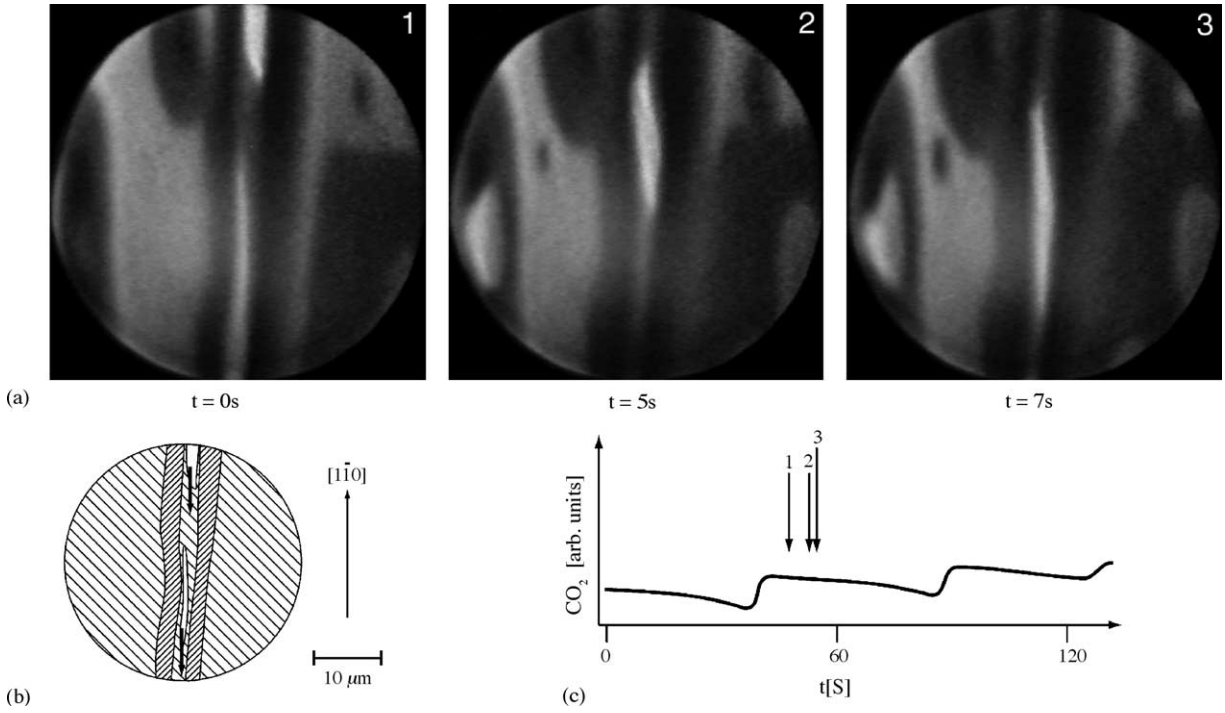

Fig. 9. Formation of a channel structure on the roughened Pt(1 1 0) surface during rate oscillations. Experimental conditions: $T = 430$ K, $p_{CO} = 5 \times 10^{-6}$ mbar, $p_{O_2} = 9.9 \times 10^{-6}$ mbar. (From ref. [53]). (a) LEEM images showing the propagation of oxygen pulses (bright elongated areas) along a single channel on each side of which are roughened CO-covered areas (two dark stripes in the center). Dark and light regions in the area outside the channel mark CO- and oxygen-covered surfaces, respectively. (b) Schematic drawing of the LEEM images in (a) in which the roughened and flat areas of the surface are indicated by different shading. Oxygen pulses move inside the channel. (c) Rate oscillations corresponding to the images in (a). Arrows mark the points where the images were taken.

4.2. Manipulation by local laser heating

A very versatile tool of influencing pattern formation on surfaces has been introduced recently [71]. By focusing a laser beam into a narrow spot of ≈80 μm diameter and the use of computer controlled galvanometer mirrors the laser spot can be moved within 1 ms to any place on the imaged area (1 mm × 2 mm) with a precision of 5 μm. Through local heating of the surface the local surface kinetics are modified. How a pulse with such a tool can be dragged across the surface is demonstrated in Fig. 11 where, after initiation of a target pattern, the laser spot was moved with constant velocity across the target pattern creating a V-shaped pulse reminiscent of a Mach cone. Initiating chemical waves by a laser pulse of course has been known for quite a long time but the versatility and the precise control allows for a rather sophisticated control of patterns on catalytic surfaces. In particular, the combination with real time imaging and the implementation of suitable feedback loops opens a wide range of possible manipulations of wave patterns (''completely addressable surface'').

4.3. Controlling turbulence

Chaotic behavior of reaction rates has been observed on single crystal surfaces as well as with polycrystalline catalysts [6,7]. A well defined transition from regular oscillation to deterministic (low-dimensional) chaos has been found in the single crystal systems Pt(1 1 0)/CO + O_2 [72], Pt(1 0 0)/NO + H_2 [73], and Pt(1 0 0)/NO + CO [22]. An experimentally verified mechanism is still lacking but a plausible model has been put forward for the NO + CO reaction on Pt(1 0 0), where the emergence of chaos has been explained by a failure of synchronizing the many nano-sized reactive 1×1 islands, which develop on the reconstructed unreactive Pt(1 0 0) surface [22]. The life-cycle of these islands needs to be synchronized via the gas phase in order to achieve macroscopic oscillations in the reaction rate. Similar problems with synchronization leading to complex time series and aperiodic behavior exist with supported noble metal catalysts [74].

Chaotic behavior involving the spatial degrees of freedom is inherently more complex and more difficult to analyze both in theory and in experiment. Theoretically quite extensive studies have been conducted with the complex Ginzburg-Landau (CGL) equation with and without the additional influence of global coupling [75,76]. Experimentally the most thoroughly studied system for chemical turbulence is clearly catalytic CO oxidation on Pt(1 1 0). The spatiotemporal chaotic behavior in this system has been characterized as spiral turbulence [77]. A similar conclusion but less well based on a statistical analysis was reached in the classification of spatiotemporal chaos in the NO + NH_3 reaction on Pt(1 0 0) [78].

Naturally, one would think that a strong global coupling would destroy chemical turbulence and would lead to a

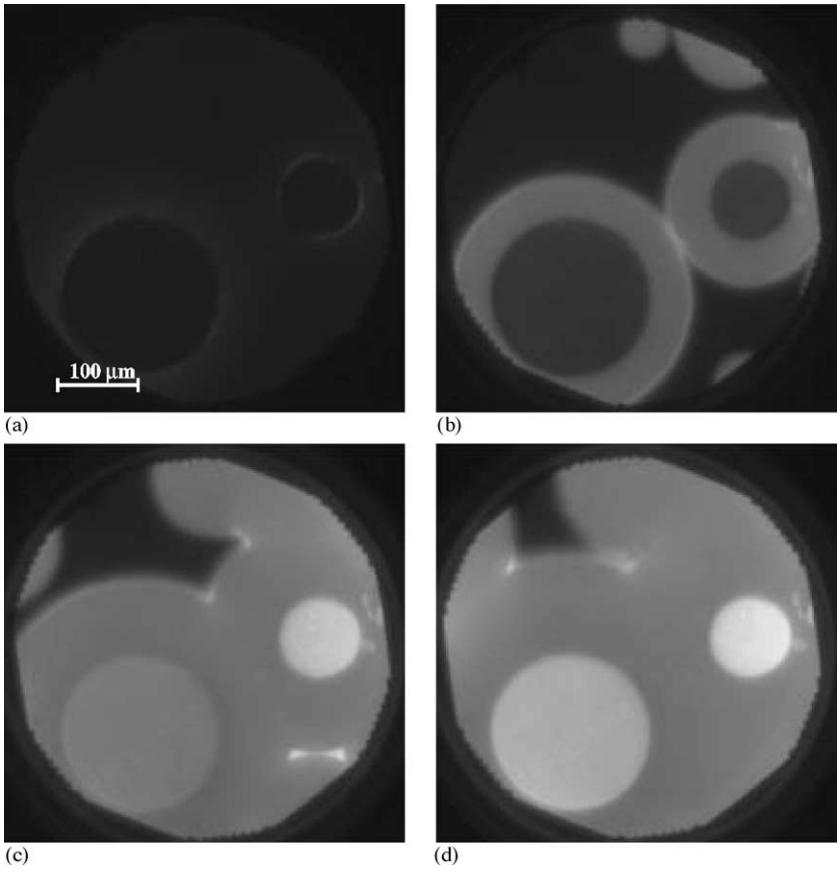

Fig. 10. PEEM images showing different stages in the titration of an oxygen saturated Pt(1 0 0 Rh microstructure with hydrogen at p_{H_2} = 1.5 × 10⁻7 mbar and T = 580 K. Inside the circles the substrate is a Pt(1 0 0) surface and the surrounding area is covered with a 500 Å thick Rh film. The bright rings surrounding the Pt domains (frame b) are reaction fronts propagating away from the interface. Images were taken at t = 0, 120, 210 and 270 s. (From ref. [60]).

synchronized oscillating state. Overall, this is in fact observed but the construction of a feedback loop between the surface changes and the forcing of an external parameter allows for an additional control parameter, given by an adjustable delay between the state of the surface and the forcing signal.

How chemical turbulence can be controlled with a suitably constructed feedback loop has been demonstrated with catalytic CO oxidation on Pt(1 1 0) [77,79]. A global signal I obtained by integrating the PEEM intensity over the imaged area was used to modulate the CO partial pressure after an adjustable delay time τ such that

$$p_{CO}(t) = p_0 + \mu[I(t-\tau) - I_0]$$

where p_0 and I_0 represent the average level of p_{CO} and the PEEM intensity and the parameter μ controls the intensity of the feedback. With such a delayed global feedback spiral turbulence could be suppressed and, depending on the reaction and feedback parameters, various types of solutions are obtained as demonstrated by Fig. 12: uniform oscillating turbulence, phase clusters, and standing waves. These examples already demonstrate the richness and the complexity of

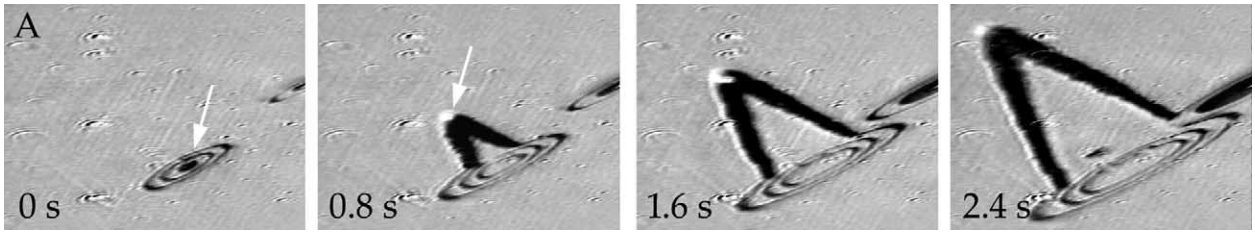

Fig. 11. Dragging an oxygen pulse across the surface with a laser spot, in the system Pt(1 1 0)/CO + O_2. After establishing excitable reaction conditions a target pattern was first initiated by local heating with the pulse. The images show an area of 1.5 mm × 1.1 mm and 1.0 mm × 0.6 mm, respectively. The arrows indicate the position of the laser spot. Experimental conditions: T = 515 K, pressure in the 10^{-4} mbar range. (From ref. [71]. Reproduced with permission of the authors).

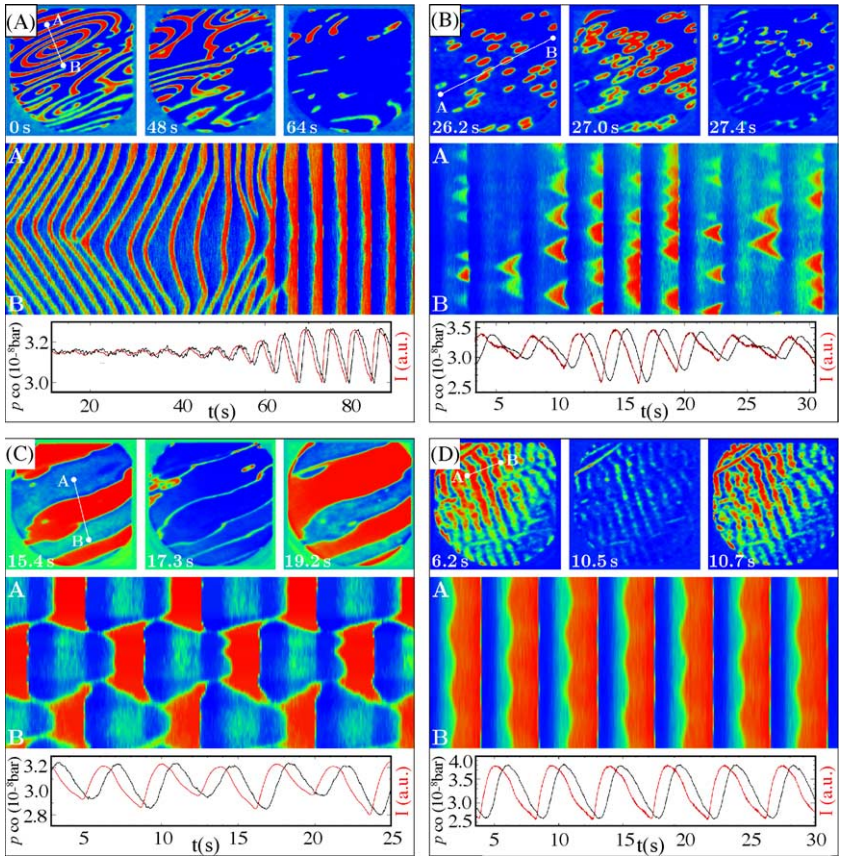

Fig. 12. Spatiotemporal patterns observed in catalytic CO oxidation on Pt(1 1 0) with global delayed feedback. (From ref. [79]. Reproduced with permission of the authors). (A) Suppression of spiral wave turbulence. (B) Intermittent turbulence. (C) Phase clusters. (D) Standing waves. In each part the upper row displays three subsequent PEEM images with a field-of-view of 500 μm in diameter, images in the middle row are space-time diagrams showing the evolution along the line *ab* indicated in the first image. Dark areas are O covered, brighter regions are mainly CO covered. The horizontal bars under each space-time diagram (bottom row) display the temporal variation of the CO partial pressure (dark line) and the variation of the integral PEEM intensity (brighter line) during the pattern evolution; the time scale is the same as in the diagram.

the phenomena that are encountered in connection with chemical turbulence on catalytic surfaces.

5. Fluctuations and nanosystems

Pattern formation and other nonlinear phenomena are not restricted to macroscopic sizes but they will also occur in ''nanoscale'' dimension systems provided that either processes exist, which fix the length scale at microscopic dimensions or that a microscopic system size is given by design or preparation. A well-known example of catalytic nanosystems are supported catalyst whose metal particle size is typically in the range of a few nm. A natural question is whether interesting nonlinear effects can be observed in such nanoscale systems.

Due to the stochastic nature of the elementary processes of adsorption, desorption, diffusion, and reaction fluctuations are naturally present in all reaction–diffusion systems [80]. If the system is sufficiently small these (internal) fluctuations, whose amplitude varies as $\frac{1}{\sqrt{N}}$ with N being the number of particles, become significant and they may eventually dominate the behavior of the system. An experimental tool that allows the in-situ imaging of a few thousand reacting particles without disturbing the imaged processes too strongly is field emission microscopy (FEM). The principle of this method and the crystallography of a Pt field emitter tip are displayed in Fig. 13. The lateral resolution of FEM of ≈20 Å, which corresponds to a few hundred adsorbed particles, is sufficiently high to be sensitive to fluctuations [81–84]. As shown by Fig. 14 the fluctuations in the bistable system Pt/CO + O_2 are strong enough to induce transitions between the two macroscopically stable branches of the reaction [81]. Another consequence of these fluctuations is that since their relative amplitude decreases with increasing system size that the bistable behavior of a catalytic reaction system vanishes below a critical size of the metal particles because then fluctuations induce transitions between the two stable branches of the kinetics. This has been demonstrated recently with nanofabricated, supported catalysts where it has been shown that the macroscopically detectable hysteresis in CO oxidation on supported Pd vanishes if the Pd particles are at or below a size of 6 nm [68].

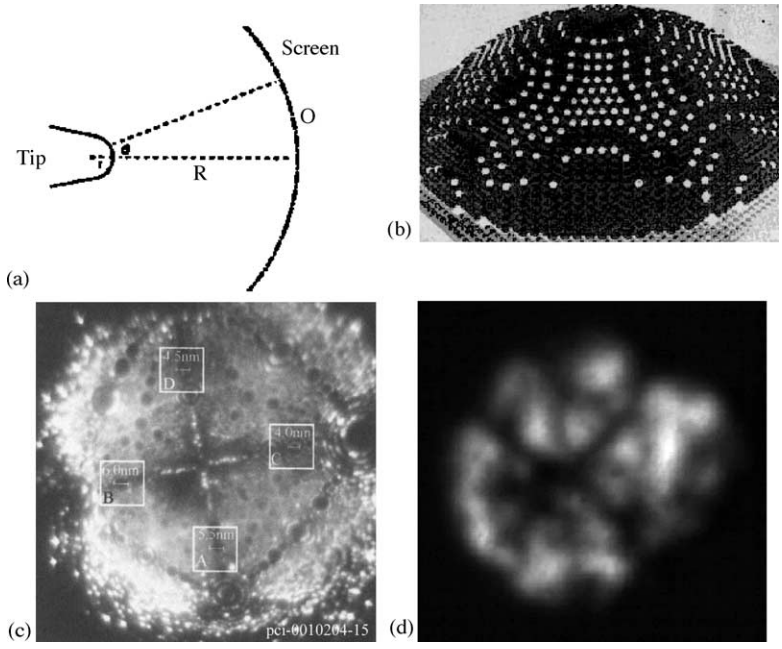

Fig. 13. Catalytic CO oxidation on a Pt field emitter tip. (From refs. [81] and [83]). (a) Schematic experimental set-up for field electron and field ion microscopy. (b) Ball model of a field emitter tip (reproduced from M.K. Miller and G.D.W. Smith, *Atom Probe Microanalysis*, publ. Materials Research Society, Pittsburgh USA, 1989). (c) FIM (=field ion microscopy) image showing the crystallography of the [1 0 0]-oriented Pt tip. The four symmetry equivalent (1 1 2) orientations used in some fluctuation studies are marked. (d) FEM image of the Pt tip under reaction conditions (T = 310 K, $p_{O_2} = 4.0 \times 10^4$ Torr, $p_{CO} = 4 \times 10^{-7}$ Torr, field strength $F = 0.4$ V Å^{-1}).

If one assumes a diffusion length of 1 μm within which the adsorbate should be well mixed then fluctuations in such an area with about 10^7–10^8 particles should still be much too small to be detected or have any significant influence on the kinetics. Such a situation is probably given in the low pressure single crystal experiments. As the pressure is increased the diffusion length should decrease due to a dense packing of the surface with adsorbates and due to a reduced lifetime of each molecule on the surface. Fluctuations within such a well mixed area should therefore increase with rising pressure. This reasoning led to the formulation of a stochastic model for CO oxidation on Pt(1 0 0) and Pt(1 1 0) [85]. Experimentally, it remains a challenging task to distinguish effects which might arise due to such fluctuations from irregularities originating from the surroundings and drifting experimental parameters.

The front width of a propagating reaction front can be approximated by $\sqrt{D\tau}$ where D is the diffusion constant of the autocatalytically produced species, which gives rise to a reaction front and τ is its average life time in the front region before it is consumed by the reaction [13]. With simple Fickian diffusion and the typical parameter values of a surface reaction the extension of the front would still be macroscopic but with energetic interactions, i.e. non-Fickian diffusion, atomically sharp interfaces can result. Such interfaces have been observed in a number of reaction systems [87,89,90].

The theoretical analysis of RD systems with energetic interactions between the species opens a wide field. Significant progress has been reached in this field in recent years as already became evident in the analysis of the patterns caused by reactive phase separation (s. Section 3.2) [86]. In surface-physics it is well known that attractive or repulsive interactions between the adparticles give rise to ordered overlayers of adsorbates conveniently summarized in 2D-phase diagrams representing thermodynamical equilibrium. In thermodynamic equilibrium of course no length scale exists but if the adsorption/desorption process of interacting particles is coupled with reaction then pattern formation in nanoscale dimensions will occur: both stationary and travelling nanostructures have been found in simulations [86].

Experimentally, the in-situ imaging of reactions on an atomic scale is still a problem. Field ion microscopy with ≈2–3 Å lateral resolution influences the reaction due to its high electric field too strongly. In scanning tunneling microscopy (STM) the STM tip also represents a severe perturbation of the system due to a geometric shielding of the surface of particles adsorbing from the gas phase and due to a tip-surface interaction. Nevertheless, this technique has been successfully employed to image reaction fronts in the $O_2 + H_2$ reaction on Pt(1 1 1) with atomic resolution as demonstrated by Fig. 15 [87,88].

6. New systems

In a series of investigations by the group of Niewenhuys oscillatory behavior in NO and N_2O reducing reactions was found over various iridium single crystal surfaces [91–93].

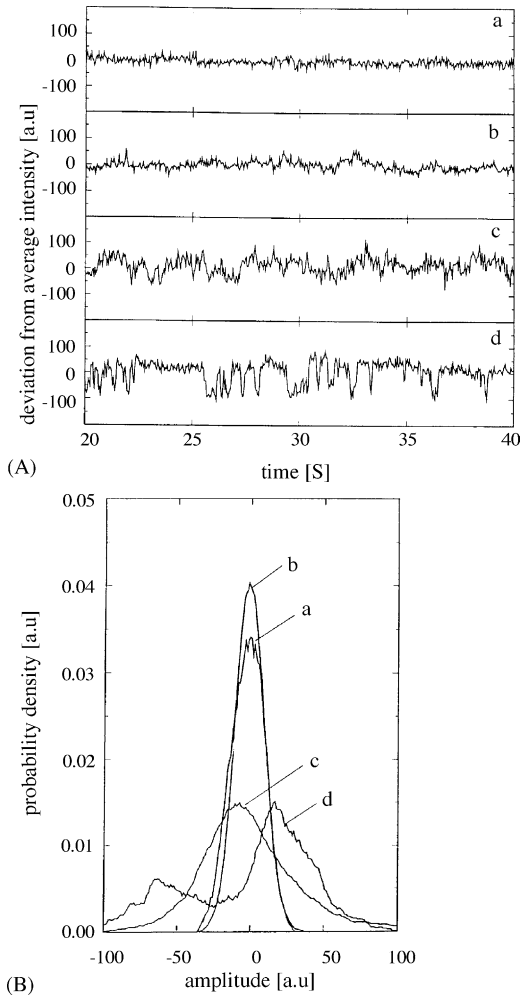

Fig. 14. Fluctuations in catalytic CO oxidation on Pt(1 1 0) under varying reaction conditions. (From ref. [81]). (A) Time series of the local (20 Å × 20 Å). FEM brightness in an area close to the (1 1 0) orientation. The data were recorded at different points of a hysteresis in T cycling experiments. (B) Probability distributions corresponding to the time series shown in (A).

Iridium surfaces represent an interesting case because on one side, the clean surfaces Ir(1 0 0) and Ir(1 1 0) exhibit reconstructions similar to Pt(1 0 0) and Pt(1 1 0), but on the other side they have a considerably higher tendency for oxide formation than Pt. Oscillations in the $NO + H_2$ reaction were found over Ir(1 1 0), Ir(2 1 0), and Ir(5 1 0) [91,92]. The latter surface, which can be written as $5 \times (1\,0\,0) \times (1\,0\,0)$, is a stepped Ir(1 0 0) surface. On Ir(5 1 0) rate oscillations occurred also in the catalytic reduction of N_2O with either H_2 or CO as reducing agent [92]. Since in-situ XPS studies of Ir(1 1 0)/$NO + H_2$ showed the rate hysteresis of this system is associated with a large hysteresis in the oxygen and nitrogen coverages, the mechanism of the rate oscillations has been attributed to a surface blockage by O_{ad} and N_{ad}, similar to Rh(1 1 0) and Rh(1 1 1) [92,93]. More details about the chemistry of these complex systems are probably required to establish an experimentally proven mechanism.

7. The pressure and material gap problem

A large body of experimental data regarding kinetic instabilities in various catalytic reactions at high pressure (mbar range to 1 bar) exists where very little information about the underlying mechanism is available. Detailed mechanistic studies were focusing almost entirely on catalytic CO oxidation [7–10]. One exception is the partial oxidation of methanol to formaldehyde over metallic copper. Rate oscillation in various reaction products were shown to be coupled to a periodic formation of Cu(I) and Cu(II) oxides showing up visibly as periodic color changes of the catalyst [94,95]. Overall, one thus has a situation similar to the well-known pressure and material gap in heterogeneous catalysis. It is by no means clear whether the results obtained with single crystals in UHV systems can be extrapolated to high-pressure conditions and polycrystalline catalysts [96].

Rate oscillations in catalytic CO oxidation at low pressure ($p < 10^{-3}$ mbar) have been shown to be due to an adsorbate induced surface phase transition in the case of the Pt surface and due to the reversible formation of subsurface oxygen in case of Pd surfaces [7,10]. For oscillations at atmospheric pressure an oxidation–reduction model has been proposed but despite its plausibility the experimental proof remains a formidable task [19]. For Pt supported on SiO_2 (average particle size 1.5 nm) in-situ X-ray diffraction showed that PtO and Pt_3O_4 are periodically formed thus proving the validity of the oxidation/reduction model for this type of catalysts [16]. With in-situ X-ray absorption spectroscopy the behavior of Pd clusters supported on carbon was studied during rate oscillations [17]. The results were interpreted as being consistent with the oxidation/reduction model though the formation of PdO was not directly visible in the data. A comparison of a Pt(1 0 0) single crystal with Pt supported on SiO_2 in the mbar range demonstrated that kinetic oscillations in catalytic CO oxidation occur on the supported catalyst in a much wider parameter space than on Pt(1 0 0)—a phenomenon attributed to coupling effects between the particles and facet orientations [97]. The extent of oxide formation under such conditions still needs to be clarified.

The question, whether beyond a certain pressure the mechanism in catalytic CO oxidation on Pt switches from the phase transition mechanism to an oxidation/reduction mechanism, is unsolved. Already, the question, whether the surface oxide which forms on Pt(1 1 0) after exposure to high p_{O2} or atomic oxygen, is difficult to answer as was demonstrated recently in a combined STM and thermal desorption study [98].

The "pressure gap" is to a large extent based on the lack of suitable in-situ techniques for high pressure conditions because the use of electrons, with which most surface analytical tools operate, restricts them typically to $p < 10^{-3}$ mbar [11]. Such restrictions do not apply for photons and, consequently, it was a great step forward in

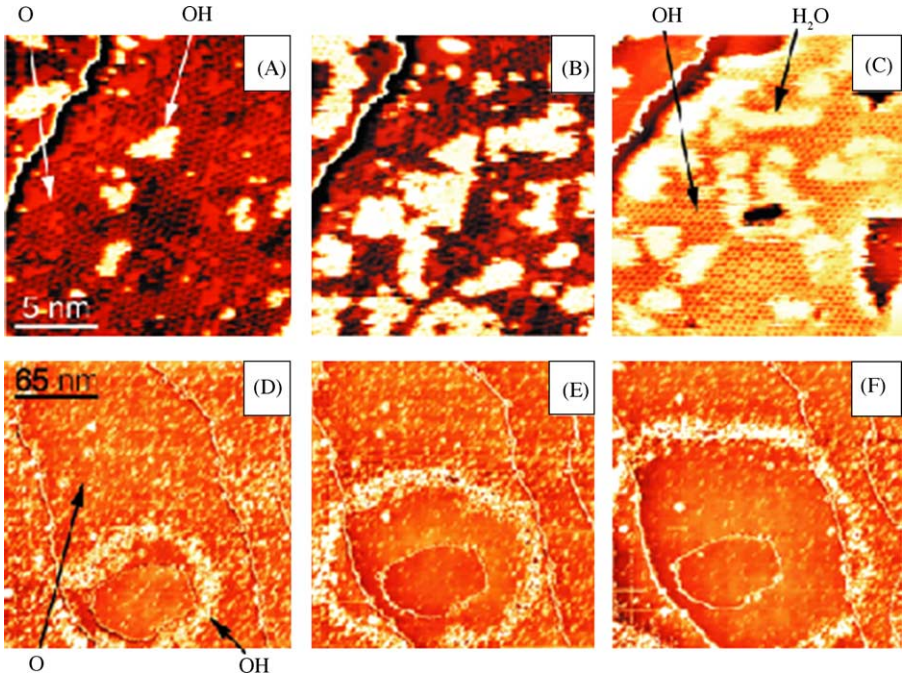

Fig. 15. Series of successive STM images, recorded during dosing of the O-covered Pt(1 1 1) surface with H_2, (A–C) Frames (17 × 17 nm) from an experiment at 131 K [$p_{H_2} = 8 \times 10^{-9}$ mbar]. The hexagonal pattern in (A) is the (2 × 2) O structure; O atoms appear as dark dots and bright features are the initial OH islands. In (C), the area is mostly covered by OH, which forms ordered ($\sqrt{3}x\sqrt{3}$) R30° and (3 × 3) structures. The white, fuzzy features are H_2O-covered areas. (D–F) Frames (220 × 220 nm) from an experiment at 112 K [$p_{H2} = 2 \times 10^{-8}$ mbar]. In (D), the surface is mostly O-covered (not resolved). The bright dots are small OH islands, most of which are concentrated in the expanding ring. H_2O in the interior of the ring is not resolved here. Thin, mostly vertical lines are atomic steps. (From ref. [88]. Reproduced with permission of the authors).

bridging the pressure gap when ellipsomicroscopy and reflection anisotropy imaging (RAM) were applied to image spatiotemporal patterns in catalytic CO oxidation on Pt(1 1 0) up into the mbar pressure range [11,99]. Both techniques, based on changes in the polarization of reflected light, are sensitive to the submonolayer range. Fig. 16 displays a raindrop-like pattern recorded with ellipsomicroscopy in the 10^{-2} mbar range [99].

What has been investigated quite in detail under atmospheric pressure conditions is the coupling between various parts of a catalyst. Under non-isothermal conditions heat waves provide the dominant coupling mode for a

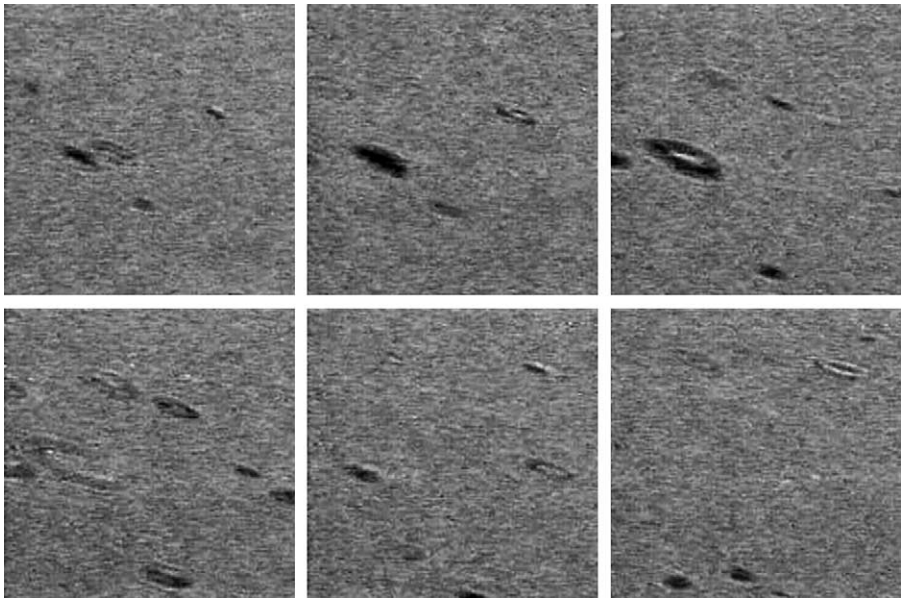

Fig. 16. Raindrop-like patterns observed with ellipsomicroscopy for surface imaging (EMSI) during catalytic CO oxidation on a Pt(1 1 0) surface in the 10^{-2} mbar range. Experimental conditions: $p_{O_2} = 2.22 \times 10^{-2}$ mbar, $p_{CO} = 5 \times 10^{-3}$ mbar, $T = 534$ K. (From ref. [94]. Reproduced with permission of the authors).

catalyst with good thermal conductivity as was shown by IR imaging [100]. For a material like zeolite loaded with Pd with a low thermal conductivity coupling via the gas phase is important for synchronization and, depending on the degree of mixing in the reaction, the coupling will be global or just non-local [101].

The difference between single crystal surfaces on one side and polycrystalline material on the other side constitutes the material gap. However, also a dynamic aspect exists, which is that all surfaces are modified by a catalytic reaction with the extent depending of course on the reaction conditions and the type of catalytic reaction [102,103]. At low p, T just a roughening of the surface may occur, which, under more drastic conditions, turns into a facetting and real morphological changes may occur. For Pt(1 1 0)/CO + O_2 it has been shown that such a roughening/facetting process is part of the oscillatory and pattern forming dynamics of the system [48–55].

The mechanistic basis of these reaction-induced substrate changes are at low p surface diffusion, step fluctuations, and adsorbate-induced surface phase transitions; at high p/high T chemical modifications, thermal etching, and chemical transport reactions are probably the dominant mechanisms. Since this catalytic etching is ubiquitous in heterogeneous catalysis it is an example where non-linear dynamics becomes vital for a proper understanding of real catalysis.

8. Conclusions and outlook

Despite the fact that the study of oscillatory effects and spatiotemporal patterns in catalytic reactions has reached a certain level of matureness – as judged from the degree of theoretical understanding and from the sophistication of the experiments – probably large areas in the field of non-linear dynamics on surfaces are still waiting to be explored. This should be true for catalysis on a nanoscale but the whole aspect of dynamics in heterogeneous catalysis has largely been neglected. The rate oscillations are so-to-speak only a kind of a special case where a synchronization mechanism produces macroscopic variations of the reaction rate. The more general case is that of some non-linear processes which take place on a local scale but are not visible to the ''outside'', since the seemingly trivial case of a stationary reaction rate is observed. Exploring such effects would demonstrate that non-linear dynamics is in fact essential for understanding heterogeneous catalysis. The development of new in-situ methods with higher spatial and temporal resolution and efforts in bridging the pressure and material gap in catalysis will help to promote such a development.

References

[1] P. Hugo, Ber. Bunsenges. Phys. Chem. 74 (1970) 121;
H. Beusch, D. Fieguth, E. Wicke, Chem. Eng. Tech. 44 (1972) 445.
[2] See early reviews on oscillating surface reactions, e.g. Refs. [3] and [4].
[3] M.G. Slinko, M.M. Slinko, Catal. Rev. Sci. Eng. 17 (1978) 119.
[4] L.F. Razón, R.A. Schmitz, Catal. Rev. Sci. Eng. 28 (1986) 89.
[5] G. Ertl, Adv. Catal. 37 (1990) 213.
[6] R. Imbihl, Prog. Surf. Sci. 44 (1993) 185.
[7] M. Eiswirth, G. Ertl, in: R. Kapral, K. Showalter (Eds.), Chemical Waves and Patterns, Kluwer, Dordrecht, 1994.
[8] F. Schüth, B.E. Henry, L.D. Schmidt, Adv. Catal. 39 (1993) 51.
[9] M.M. Slinko, N. Jaeger, Oscillatory Heterogeneous Catalytic Systems, Studies in Surface Science and Catalysis, vol. 86, Elsevier, Amsterdam, 1994.
[10] R. Imbihl, G. Ertl, Chem. Rev. 95 (1995) 697.
[11] H.H. Rotermund, Surf. Sci. Rep. 29 (1997) 265.
[12] See also the focus issues of Chaos 12/1 (2002) and of the N. J. Phys. 5 (2003).
[13] A.S. Mikhailov, Foundations of Synergetics I, Springer, Berlin, 1994;
A.S. Mikhailov, A.Yu. Loskutov, Foundations of Synergetics II. Chaos and Noise, second revised ed., Springer, Berlin, 1996.
[14] R. Kapral, K. Showalter (Eds.), Chemical Waves and Patterns Kluwer, Dordrecht, 1994.
[15] M.P. Cox, G. Ertl, R. Imbihl, J. Rüstig, Surf. Sci. 134 (1984) L517.
[16] N. Hartmann, R. Imbihl, W. Vogel, Catal. Lett. 28 (1994) 373.
[17] T. Ressler, M. Hagelstein, U. Hatje, W. Metz, J. Phys. Chem. B 101 (1997) 6680.
[18] S. Ladas, R. Imbihl, G. Ertl, Surf. Sci. 219 (1989) 88.
[19] B.C. Sales, J.E. Turner, M.B. Maple, Surf. Sci. 114 (1982) 381.
[20] T. Fink, J.-P. Dath, R. Imbihl, G. Ertl, J. Chem. Phys. 95 (1991) 2109.
[21] A. Hopkinson, J.M. Bradley, X.-C. Guo, D.A. King, Phys. Rev. Lett. 71 (1993) 1597.
[22] N. Khrustova, G. Veser, A.S. Mikhailov, R. Imbihl, Phys. Rev. Lett. 75 (1995) 3564;
N. Khrustova, A.S. Mikhailov, R. Imbihl, J. Chem. Phys. 107 (1997) 2096.
[23] A. Hopkinson, D.A. King, Chem. Phys. 177 (1993) 433.
[24] S.J. Lombardo, T. Fink, R. Imbihl, J. Chem. Phys. 98 (1993) 5526.
[25] F. Mertens, R. Imbihl, Nature 370 (1994) 124.
[26] F. Mertens, S. Schwegmann, R. Imbihl, J. Chem. Phys. 106 (1997) 4319.
[27] A. Schaak, R. Imbihl, Chem. Phys. 107 (1997) 4741.
[28] A. Makeev, M. Hinz, R. Imbihl, J. Chem. Phys. 114 (2001) 9083.
[29] M. Falcke, H. Engel, J. Chem. Phys. 101 (1994) 6255;
H. Levine, X. Zou, Phys. Rev. Lett. 66 (1992) 204.
[30] A.v. Oertzen, H.H. Rotermund, A.S. Mikhailov, G. Ertl, J. Phys. Chem. B 104 (2000) 3155.
[31] K.C. Rose, D. Battogtokh, A.S. Mikhailov, R. Imbihl, W. Engel, A.M. Bradshaw, Phys. Rev. Lett. 76 (1996) 3582.
[32] N. Hartmann, S. Shaikhutdinov, A. Schaak, R. Imbihl, Surf. Sci. 548 (2004) 163.
[33] A. Schaak, R. Imbihl, J. Chem. Phys. 116 (2002) 9021;
A. Schaak, R. Imbihl, J. Chem. Phys. 113 (2000) 9822.
[34] M.I. Monine, A. Schaak, B.Y. Rubinstein, R. Imbihl, L.M. Pismen, Cat. Today 70 (2001) 321.
[35] J. Lauterbach, K. Asakura, H.H. Rotermund, Surf. Sci. 313 (1994) 52;
A.v. Oertzen, A. Mikhailov, H.H. Rotermund, G. Ertl, Surf. Sci. 350 (1996) 259.
[36] A. Schaak, R. Imbihl, Chem. Phys. Lett. 283 (1998) 386;
M. Monine, L.M. Pismen, M. Bär, M. Or-Guil, J. Chem. Phys. 117 (2002) 4473.
[37] J. Wider, T. Greber, E. Wetli, T.J. Kreutz, P. Schwaller, J. Osterwalder, Surf. Sci. 417 (1998) 301.3.
[38] O. Kortlüke, V.N. Kuzovkov, W. von Niessen, Phys. Rev. Lett. 83 (1999) 3089.
[39] M. Kiskinova, Poisoning and Promotion in Catalysis Based on Surface Science Concepts, Elsevier, 1992.

[40] H. Marbach, S. Günther, B. Luerssen, L. Gregoratti, M. Kiskinova, R. Imbihl, Catal. Lett. 83 (2002) 161.
[41] H. Marbach, M. Hinz, S. Gunther, L. Gregoratti, M. Kishkinova, R. Imbihl, Chem. Phys. Lett. 364 (2002) 207.
[42] H. Marbach, S. Günther, T. Neubrand, R. Hoyer, L. Gregoratti, M. Kiskinova, R. Imbihl, J. Phys. Chem. 108 (2004) 15182.
[43] Y. De Decker, H. Marbach, M. Hinz, S. Günther, M. Kiskinova, A.S. Mikhailov, R. Imbihl, Phys. Rev. Lett. 92 (2004) 198305;
M. Hinz, R. Imbihl, J. Phys. Chem. B 108 (2004) 14620.
[44] Y. De Decker, A.S. Mikhailov, J. Phys. Chem. B 108 (2004) 14765.
[45] S. Günther, H. Marbach, R. Hoyer, R. Imbihl, L. Gregoratti, A. Barinov, M. Kiskinova, J. Chem. Phys. 117 (2002) 2923.
[46] H. Marbach, Thesis, Hannover, 2002.
[47] H. Marbach, S. Günther, T. Neubrand, R. Imbihl, Chem. Phys. Lett. 349 (2004) 64.
[48] S. Ladas, R. Imbihl, G. Ertl, Surf. Sci. 197 (1988) 153;
S. Ladas, R. Imbihl, G. Ertl, Surf. Sci. 198 (1988) 42.
[49] J. Falta, R. Imbihl, M. Henzler, Phys. Rev. Lett. 64 (1990) 1409.
[50] R. Imbihl, A.E. Reynolds, D. Kaletta, Phys. Rev. Lett. 67 (1991) 275.
[51] R. Imbihl, Modern Phys. Lett. B 6 (1992) 493.
[52] M.I. Monine, L. Pismen, R. Imbihl, J. Chem. Phys. 121 (2004) 11332.
[53] K.C. Rose, B. Berton, R. Imbihl, W. Engel, A.M. Bradshaw, Phys. Rev. Lett. 79 (1997) 3427.
[54] F. Meißen, A.J. Patchett, R. Imbihl, A.M. Bradshaw, Chem. Phys. Lett. 336 (2001) 181.
[55] H. Wei, G. Lilienkamp, R. Imbihl, Chem. Phys. Lett. 389 (2004) 284.
[56] M.D. Graham, I.G. Kevrekidis, K. Asakura, J. Lauterbach, K. Krischer, H.H. Rotermund, G. Ertl, Science 264 (1994) 80.
[57] For wave references, the reader is referred to Refs. [58] and [59].
[58] X. Li, I.G. Kevrekidis, M. Pollmann, A.G. Papathanasiou, H.H. Rotermund, Chaos 12 (2002) 190.
[59] R. Imbihl, Chaos 12 (2002) 182.
[60] E. Schütz, N. Hartmann, I.G. Kevrekidis, R. Imbihl, Catal. Lett. 54 (1998) 181.
[61] S.Y. Shvartsman, I.G. Kevrekidis, E. Schütz, R. Imbihl, Phys. Rev. Lett. 83 (1999) 2857.
[62] M. Pollmann, H.H. Rotermund, G. Ertl, X. Li, I.G. Kevrekidis, Phys. Rev. Lett. 86 (2001) 6038.
[63] J. Lauterbach, K. Asakura, P.B. Rasmussen, H.H. Rotermund, M. Bär, M.D. Graham, I.G. Kevrekidis, G. Ertl, Physica D 123 (1998) 493.
[64] G. Haas, M. Bär, I.G. Kevrekidis, H.H. Rotermund, G. Ertl, Phys. Rev. Lett. 75 (1995) 3560.
[65] N. Hartmann, M. Bär, I.G. Kevrekidis, K. Krischer, R. Imbihl, Phys. Rev. Lett. 76 (1996) 1384.
[66] J. Christoph, M. Bär, M. Eiswirth, N. Hartmann, I.G. Kevrekidis, R. Imbihl, Phys. Rev. Lett. 82 (1999) 1586.
[67] E. Schütz, F. Esch, S. Günther, A. Schaak, M. Marsi, M. Kiskinova, R. Imbihl, Catal. Lett. 63 (1999) 13.
[68] V. Johanek, M. Laurin, A.W. Grant, B. Kasemo, C.R. Henry, J. Libuda, Science 304 (2004) 1639.
[69] J. Liu, E. Sheina, T. Kowalewski, R.D. McCullough, Ang. Chem. Int. Ed. 41 (2002) 329.
[70] M. Kiskinova, E. Di Fabrizio, M. Gentili, M. Marsi, Surf. Rev. Lett. 6 (1999) 265.
[71] J. Wolff, A.G. Papathanasiou, I.G. Kevrekidis, H.H. Rotermund, G. Ertl, Science 294 (2001) 134.
[72] M. Eiswirth, K. Krischer, G. Ertl, Surf. Sci. 202 (1988) 565.
[73] P.D. Cobden, J. Siera, B.E. Nieuwenhuys, J. Vac. Sci. Technol. A 10 (1992) 2487.
[74] M.M. Slinko, A.A. Ukharskii, N.V. Peskov, N.I. Jaeger, Catal. Today 70 (2001) 341.
[75] D. Battogtokh, A.S. Mikhailov, Physica D 90 (1996) 84;
D. Battogtokh, A. Preusser, A.S. Mikhailov, Physica D 106 (1997) 327.
[76] F. Mertens, R. Imbihl, A.S. Mikhailov, J. Chem. Phys. 99 (1993) 8668;
F. Mertens, R. Imbihl, A.S. Mikhailov, J. Chem. Phys. 101 (1994) 9903.
[77] M. Bertram, Thesis, TU Berlin, 2002.
[78] I.M. Irurzun, R. Imbihl, J.L. Vicente, E.E. Mola, Chem. Phys. Lett. 389 (2004) 212.
[79] M. Kim, M. Bertram, M. Pollmann, A. von Oertzen, A.S. Mikhailov, H.H. Rotermund, G. Ertl, Science 292 (2001) 1357.
[80] N.G. van Kampen, Stochastic Processes in Physics and Chemistry, North Holland, Amsterdam, 1987.
[81] Y. Suchorski, J. Beben, E.W. James, J.W. Evans, R. Imbihl, Phys. Rev. Lett. 82 (1999) 1907.
[82] Y. Suchorski, J. Beben, R. Imbihl, E.W. James, D.-J. Liu, J.W. Evans, Phys. Rev. B 63 (2001) 165417.
[83] R. Imbihl, N. J. Phys. 5 (2003) 62.
[84] N. Pavlenko, J.W. Evans, D.-J. Liu, R. Imbihl, Phys. Rev. E 65 (2001) 16121.
[85] C. Reichert, J. Starke, M. Eiswirth, J. Chem. Phys. 115 (2001) 4829.
[86] M. Hildebrand, A.S. Mikhailov, J. Phys. Chem. 100 (1996) 19089;
M. Hildebrand, A.S. Mikhailov, Phys. Rev. Lett. 81 (1998) 2602;
A.S. Mikhailov, Chaos 12 (2002) 144.
[87] S. Völkening, K. Bedürftig, K. Jacobi, J. Wintterlin, G. Ertl, Phys. Rev. Lett. 83 (1999) 2672.
[88] C. Sachs, M. Hildebrand, S. Völkening, J. Wintterlin, G. Ertl, Science 293 (2001) 1635.
[89] V. Gorodetskii, J. Lauterbach, H.H. Rotermund, J.H. Block, G. Ertl, Nature 370 (1994) 277.
[90] M.F.H. van Tol, A. Gielbert, B.E. Nieuwenhuys, Catal. Lett. 16 (1992) 297.
[91] C.A. de Wolf, B.E. Niewenhuys, Cat. Today 70 (2001) 287.
[92] S.A.C. Carabineiro, W.D. van Noort, B.E. Niewenhuys, Catal. Lett. 84 (2002) 135.
[93] C.A. de Wolf, et al. J. Phys. Chem. B 105 (2001) 4254.
[94] H. Werner, D. Herein, G. Schulz, U. Wild, R. Schlögl, Catal. Lett. 49 (1997) 109.
[95] A. Amariglio, O. Benali, H. Amariglio, J. Catal. 118 (1989) 164.
[96] D.J. Dwyer, F.M. Hoffmann (Eds.), Surface Science of Catalysis, ACS Symposium Series, vol. 482, American Chemical Society, Washington, 1992.
[97] T. Lele, J. Lauterbach, Chaos 12 (2002) 164.
[98] W.X. Li, L. Österlund, E.K. Vestergaard, R.T. Vang, J. Matthiesen, T.M. Pedersen, E. Laegsgaard, B. Hammer, F. Besenbacher, Phys. Rev. Lett. 93 (2004) 146101–146104.
[99] H.H. Rotermund, G. Haas, R.U. Franz, R.M. Tromp, G. Ertl, Science 270 (1995) 608.
[100] S.Y. Yamamoto, C.M. Surko, M.B. Maple, R.K. Pina, Phys. Rev. Lett. 74 (1995) 4071;
D. Luss, B. Marwaha, Chaos 12 (2002) 172.
[101] M.M. Slinko, A.A. Ukharskii, N. Jaeger, PCCP 3 (2001) 1015.
[102] M. Flytzani-Stephanopoulos, L.D. Schmidt, Prog. Surf. Sci. 9 (1979) 83.
[103] T.C. Wei, J. Phillips, Adv. Catal. 41 (1992) 359.